Liquid Ammonia Mediated Metathesis: Synthesis of Binary Metal Chalcogenides and Pnictides

G. A. Shaw and I. P. Parkin*

Department of Chemistry, Christopher Ingold Laboratories, University College London, 20 Gordon Street, London, U.K., WC1H 0AJ

Received June 18, 2001

Addition of stoichiometric amounts of low valent metal halides to liquid ammonia solutions of disodium chalcogenide (Na_2E; E = S, Se, Te) afforded a range of both crystalline (PbE (E = S, Se, Te), TlE (E = S, Se), Tl_5Te_3, Ag_2E (E = S, Se, Te)) and X-ray amorphous (MS (M = Ni, Cu, Zn, Cd, Hg), M_2E_3 (M = Ga, In; E = S, Se, Te), HgE (E = Se, Te), CuE (E = S, Se, Te), Cu_2S) metal chalcogenides in good yield (95%). Reactions between metal halides and sodium pnictides (Na_3Pn; Pn = As, Sb) in liquid ammonia also afforded X-ray amorphous material (M_3Pn_2, M = Zn, Cd; MPn, M = Fe, Co, Ni) in good yield (95%). Isolation of the metal chalcogenides and pnictides was achieved through washing with CS_2 and distilled water. All reactions were complete within 36 h. Products were characterized by X-ray powder diffraction (XRD), scanning electron microscopy (SEM), energy-dispersive X-ray analysis (EDXA), electron probe analysis, FT-IR spectroscopy, Raman spectroscopy, microanalysis, and band gap measurements. Annealing amorphous material at 250−300 °C for 48 h induced sufficient crystallinity for analysis by X-ray powder diffraction.

Introduction

Binary metal chalcogenides function as catalysis, secondary batteries, lubricants, and semiconductors.[1] Band gap energies of group 12−16 materials are important for the emission, detection, and modulation of light in the visible and near-UV regions;[2] group 13−15 materials are suitable for red to near-IR radiation. Applications include coatings, gratings,[3] and a wide range of optical windows.[4] Group 13−16 materials fall into two different compound types—M_2E_3 and ME (M = Ga, In; E = S, Se, Te); both materials are direct band gap semiconductors and of interest as photovoltaic and optoelectronic materials. Gallium and indium sesquichalcogenides (M_2E_3) have a wide band gap, offering an alternative to group 12−16 materials.[4] Catalytic activity of transition metal sulfides is well documented; for example, MoS_2 is used as a petrochemical catalyst.[5] The disulfides of tin, titanium, molybdenum, zirconium, and hafnium all crystallize as two-dimensional lattices exhibiting weak interlayer bonding and find commercial applications as high-temperature lubricants,[3] battery cathodes,[2,3] and hydrodesulfurization catalysts.[6] The sulfides and selenides of zinc and cadmium are used in reflective coatings, as well as in the pigmentation of paints, rubber, and porcelain.[3,7]

Various established syntheses exist for the preparation of bulk binary chalcogenides. These include reaction of silyl sulfides,[8] sol−gel processing,[9] electrodeposition from solution,[10] decomposition of precursors,[11] and elemental combination reactions at elevated temperature.[12] Recent work has focused on the synthesis of nanoparticulate chalcogenides and has used confined environments such as zeolites and micelles to restrict particle size.[13] We have shown that traditional elemental combination reactions can be improved by utilizing liquid ammonia as solvent.[14] Some elemental metals react with chalcogenide/ammonia solutions to form crystalline metal chalcogenides at room temperature.[15] The reactions often form single-phase materials in common mineral modifications but were, however, restricted to chalcophilic metals such as Zn, Cd, Hg, Ag, Pb, and Sn. Self-propagating elemental combination reactions have also been used to form metal sulfides in a process known as SHS (self-propagating high-temperature synthesis).[16]

SHS is a process that utilizes highly exothermic reactions to obtain a sustainable combustion wave.[17] The reaction becomes self-propagating, thereby greatly reducing processing time and

* To whom correspondence should be addressed.

(1) (a) Lewis, K. L.; Savage, J. A.; Marsh, K. J.; Jones, A. P. C. New Optical Materials. *Proc. SPIE-Int. Soc. Opt. Eng.* **1983**, *400*, 21. (b) Kilbourne, B. T. *A Lanthanide Lanthology- Part 1*; Molycorp Inc.: White Plains, NY, 1993.
(2) Nicolau, Y. F.; Dupuy, M.; Brunel, M. *J. Electrochem. Soc.* **1990**, *137*, 2915.
(3) Greenwood, N. N.; Earnshaw, E. A. *Chemistry of the Elements*; Pergamon Press: Oxford, 1990; pp 1403−6.
(4) O'Brien, P.; Ryôki, J. *J. Mater. Chem.* **1995**, *5*, 1761.
(5) Tsigdinos, G. A.; Moh, G. W. *Aspects of Molybdenum and Related Chemistry*; Springer: New York, 1978; Vol. 76.
(6) Hasse, M. A.; Qiu, J.; DePuydt J. M.; Cheng, H. *Appl. Phys. Lett.* **1991**, *59*, 1272.
(7) Fielder, I.; Bayard, M. *Artists Pigments, A Handbook of their History and Characteristics*; Feller, R. L., Ed.; Cambridge University Press: Cambridge, 1986; Vol. 1, p 65.
(8) Schleich, D. M.; Martin, M. J. *J. Solid State Chem.* **1986**, *64*, 359.
(9) Sriram, M. A.; Kumta, P. N. *J. Mater. Chem.* **1998**, *8*, 2453.
(10) Massacces, S.; Sanchez, S.; Vedel, J. *J. Electroanal. Chem.* **1996**, *412*, 95. Bensalem, R.; Schleich, D. M. *Mater. Res. Bull.* **1988**, *23*, 857.
(11) Nomura, R.; Konishi, K.; Futenma, S.; Matsuda, H. *Appl. Organomet. Chem.* **1990**, *4*, 607.
(12) Coustal, R. *J. Chim. Phys.* **1931**, *31*, 277. Braver, G. *Handbook of Preparative Inorganic Chemistry*, 2nd ed.; Academic Press: New York, 1965; Vols. 1, 2.
(13) (a) Petit, C.; Pileni, M. P. *J. Phys. Chem.* **1988**, *92*, 2282. (b) Lianos, P.; Thomas, J. K. *Chem Phys. Lett.* **1986**, *125*, 299. (c) Wang, Y.; Herron, N. *J. Phys. Chem.* **1987**, *91*, 257.
(14) (a) Henshaw, G.; Shaw, G. A.; Hector, A.; Parkin, I. P. *Main Group Metal Chem.* **1996**, *1*, 183. (b) Parkin, I. P.; Henshaw, G.; Shaw, G. A. *J. Mater. Sci. Lett.* **1996**, *15*, 1741. (c) Omar, B.; Parkin, I. P.; Shaw, G. A. *J. Chem. Soc., Dalton Trans.* **1997**, *9*, 1385.
(15) (a) Parkin, I. P.; Shaw G. A.; Henshaw, G *J. Chem. Soc., Dalton Trans.* **1997**, 231. (b) Parkin, I. P. Henshaw, G.; Shaw, G. A. *J. Chem. Soc., Chem. Commun.* **1996**, 1095.
(16) Merzhanov, A. G. *Russ. Chem. Bull.* **1997**, *1*, 8.
(17) Crider, J. F. *Ceram. Eng. Sci. Proc.* **1982**, *3* (9−10), 519.

10.1021/ic010648s CCC: $20.00
Published on Web 12/06/2001

Table 1. XRD Data for Crystalline Binary Transition Metal Chalcogenides Synthesized by Metathetical Reactions in Liquid Ammonia at Room Temperature

reagents[a]	products formed from reaction (identified by XRD)[b]	product color	phases obtained after annealing washed mater	lattice params, Å (± 0.01)	lit.[36] lattice params, Å
$2AgF + Na_2S$	Ag_2S (acanthite) + NaF	black	Ag_2S (acanthite)	$a = c = 4.48$	$a = c = 4.46$
$2AgF + Na_2Se$	Ag_2Se (naumannite) + NaF	black	Ag_2S (naumannite)	$a = 4.33$, $b = 7.06$, $c = 7.76$	$a = 4.33$, $b = 7.06$, $c = 7.76$
$2AgF + Na_2Te$	Ag_2Te (hessite) + NaF	black	Ag_2S (acanthite)	$a = 8.07$, $b = 4.47$, $c = 8.94$	$a = 8.09$, $b = 4.47$, $c = 8.96$
$2TlCl + Na_2S$	$Tl[TlS_2]$ + NaCl	black	$Tl[TlS_2]$	$a = 7.79$, $c = 6.80$	$a = 7.79$, $c = 6.80$
$TlCl + Na_2Se$	$Tl[TlSe_2]$ + NaCl	black	$Tl[TlSe_2]$	$a = 8.02$, $c = 7.00$	$a = 8.02$, $c = 7.00$
$2TlCl + Na_2Te$	Tl_5Te_3 + NaCl	black	Tl_5Te_3	$a = 8.93$, $c = 12.62$	$a = 8.92$ (5), $c = 12.61$ (5)
$PbCl + Na_2S$	PbS (galena) + NaCl	black	PbS (galena)	$a = c = 5.93$	$a = c = 5.93$
$PbCl + Na_2Se$	PbSe (clausthalite) + NaCl	black	PbSe (clausthalite)	$a = c = 6.12$	$a = c = 6.12$
$PbCl + Na_2Te$	PbTe (altaite) + NaCl	black	PbTe (altaite)	$a = c = 6.46$	$a = c = 6.46$

[a] Reagents (expressed with molar ratios) stirred in liquid ammonia at room temperature for 36 h. [b] Phases characterized by X-ray powder diffraction *prior* to workup of reaction product.

Table 2. XRD Data for Amorphous Binary Transition Metal Chalcogenides Synthesized by Metathetical Reactions in Liquid Ammonia at Room Temperature

reagents[a]	prewash mater	product color	phases obtained after annealing washed mater[b]	lattice params, Å (± 0.01)	lit. lattice params,[36] Å
$NiCl_2 + Na_2S$	NaCl	black	NiS (millerite)	$a = c = 3.42$	$a = c = 3.42$
$ZnCl_2 + Na_2S$	NaCl	yellow	ZnS (wurzite)	$a = 3.82$, $c = 6.25$	$a = 3.82$, $c = 6.26$
$CdCl_2 + Na_2S$	NaCl	yellow	CdS (greenockite)	$a = 4.14$, $c = 6.72$	$a = 4.14$, $c = 6.72$
$2CuBr + Na_2S$	NaBr	black	Cu_2S (chalcocite) + [$Cu_{1.8}S$, $Cu_{1.9}S$]	$a = 3.96$, $c = 6.78$	$a = 3.96$, $c = 6.78$
$CuCl_2 + Na_2S$	NaCl	black	CuS (covelite) $Cu_{1.8}S$ (diginite)	$a = 3.76$, $c = 16.21$ M[c]	$a = 3.76$, $c = 16.19$
$CuCl_2 + Na_2Se$	NaCl	black	CuSe (klockmannite) + [$CuSe_2$ (krutaite)]	$a = 3.93$, $c = 17.20$	$a = 3.93$, $c = 17.22$
$CuCl_2 + Na_2Te$	NaCl	black	$Cu_{2.72}Te_2 + Cu_4Te_3$	M[c]	
$HgCl_2 + Na_2S$	NaCl	black	β-HgS (metacinnebar)	$a = c = 5.85$	$a = c = 5.85$
$HgCl_2 + Na_2Se$	NaCl	black	HgSe (tiemannite)	$a = c = 6.08$	$a = c = 6.07$
$HgCl_2 + Na_2Te$	NaCl	black	HgTe (coloradoite)	$a = c = 6.46$	$a = c = 6.45$
$2GaCl_3 + 3Na_2S$	NaCl	black	Ga_2S_3	$a = 3.68$, $c = 6.03$	$a = 3.68$, $c = 6.03$
$2GaCl_3 + 3Na_2Se$	NaCl	black	Ga_2Se_3	$a = 6.66$, $c = 11.65$	$a = 6.66$, $c = 11.65$
$2GaCl_3 + 3Na_2Te$	NaCl	black	Ga_2Te_3	$a = c = 5.90$	$a = c = 5.90$
$2InCl_3 + 3Na_2S$	NaCl	black	In_2S_3	$a = c = 10.78$	$a = c = 10.78$
$2InCl_3 + 3Na_2Se$	NaCl	black	In_2Se_3	$a = 7.12$, $c = 19.37$	$a = 7.12$, $c = 19.37$
$2InCl_3 + 3Na_2Te$	NaCl	black	In_2Te_3	$a = c = 18.51$	$a = c = 18.49$

[a] Reagents (expressed with molar ratios) stirred in liquid ammonia at room temperature for 36 h. [b] Phases characterized by X-ray powder diffraction *after* annealing at 250−300 °C for 48 h. All minor phases (< ca. 10%) represented by square brackets. [c] M = matched stick pattern to database standard.

applied energy when compared to conventional sintering.[18] However, high reaction rates also result in a lack of control of grain size and density.[19] Calculated adiabatic reaction temperatures for such reactions often exceed 1525 °C,[20] restricting them to the synthesis of refractory transition metal dichalcogenides: MoS_2, NbS_2, WSe_2, and $TaSe_2$.[21]

A variant of SHS has been developed by R. Kaner's group[22] and ourseleves[23] and is known as solid-state metathesis, SSM.[22] This new reaction type has been primarily undertaken in ampules or sealed containers. It involves the reaction of metal halides with alkali metal chalcogenides and pnictides, eq 1. The driving force for the reaction is the co-formation of a salt along with the desired metal chalcogenide.

$$MCl_4 + 2Na_2E \rightarrow ME_2 + 4NaCl \qquad (1)$$

Maximum reaction temperature can be controlled to some extent in SSM by altering the co-formed salt. Solid state metathesis reaction of anhydrous metal chlorides with sodium sulfide yielded a range of transition metal, lanthanide, actinide, and main-group metal chalcogenides.[23] Reactions were initiated thermally inside a heated sealed ampule,[24] by a heated filament, known as point source initiation,[25] by mechanical grinding of low melting point solids,[26] or by simple mixing of highly volatile components at room temperature.[27] SSM reactions often initiate at relatively low temperatures and are frequently self-propagating. Total heat of formation of the product mixture is frequently in excess of ca. 250 kcal/mol^{-1} generating temperatures exceeding 1000 °C. The reactions once initiated are extremely rapid (1−5 s)[23] and often associated with the emission of clouds of vaporized co-formed salt. Unlike many precursor reactions, these byproduct salts are highly ionic in character and so are easily removed from the markedly less ionic metal sulfide (to <0.01%)[24] simply by trituration with a suitable solvent such as water, THF, or methanol. It is the formation and subsequent melting of this coproduced salt that ultimately gives control of

(18) Munir, Z. A.; Anselmi-Tamburini, U. *Mater. Sci. Rep.* **1989**, *3* (7−8), 277.
(19) Rice, R. W.; McDonough, W. J. *J. Am. Ceram. Soc.* **1985**, *68* (5), C122.
(20) Novikov, N. P.; Borovinskaya, I. P.; Merzhanov, A. G. *Combustion processes in chemical technology and metallurgy*; Russ. Acad. Sci.: Chernogolovka, 1975; p 174.
(21) (a) Sheppard, L. M. *Adv. Mater. Process.* **1986**, *2*, 25−32. (b) Moore, J. J.; Feng, H. J. *Prog. Mater. Sci.* **1995**, *39*, 243.
(22) Bonneau, P. R.; Shibao, R. K.; Kaner, R. B. *Inorg. Chem.* **1990**, *29*, 2511.
(23) Parkin, I. P. *Chem. Soc. Rev.* **1996**, 199.
(24) (a) Fitzmaurice, J. C.; Hector, A. L.; Parkin, I. P. *J. Chem. Soc., Dalton Trans.* **1993**, 2435. (b) Fitzmaurice, J. C.; Hector, A. L.; Parkin, I. P. *Polyhedron* **1993**, *12*, 1295.
(25) Treece, R. E.; Conklin, J. A.; Kaner, R. B. *Inorg. Chem.* **1994**, *33*, 5701.
(26) Treece, R. E.; Macala, G. S.; Kaner, R. B. *Chem. Mater.* **1992**, *4*, 9.
(27) Hector, A. L.; Parkin, I. P. *J. Chem. Soc., Chem. Commun.* **1993**, 1096.

the reaction temperature since it is the molten salt that sustains the propagation wave.

Recent developments in SSM have included the synthesis of binary main-group pnictide materials,[23,28] as well as conducting the process in mediating solvents. These have included both toluene[29] and diglyme solvents.[28] The reaction proceeds either in solution or at a solution−solid interface. To date gallium, cobalt, and nickel pnictides[28] and titanium chalcogenides[29] have been synthesized by solution-phase metathesis.

We report here the synthesis of a wide range of binary chalcogenide and pnictide materials by metathetical reactions in liquid ammonia. This process enables isolation of crystalline nanoscaled materials. The new route also offers an advantage over conventional SSM reactions in that the reactions occur essentially at room temperature, thus allowing synthesis of products with minimal thermal defects.

Results

Binary Metal Chalcogenides: Synthesis and Characterization. Addition of stoichiometric amounts of metal halides to liquid ammonia solutions of disodium chalcogenide at room temperature afforded a range of both crystalline (Table 1, eqs 2−5) and X-ray amorphous (Table 2, eqs 6−11) metal chalcogenides in good yield, ca. 95%. Reactions were completed within 36 h.

$$PbCl_{2(s)} + Na_2E \rightarrow PbE_{(s)} + 2NaCl_{(s)}\ (E = S, Se, Te) \quad (2)$$

$$2AgF_{(s)} + Na_2E \rightarrow Ag_2E_{(s)} + 2NaF_{(s)}\ (E = S, Se, Te) \quad (3)$$

$$4TlCl_{(s)} + 2Na_2E_{(am)} \rightarrow Tl[TlE_2]_{(s)} + 2Tl_{(s)} + 2NaCl_{(s)}\ (E = S, Se) \quad (4)$$

$$6TlCl_{(s)} + 3Na_2Te_{(s/am)} \rightarrow Tl_5Te_{3(s)} + 2NaCl_{(s)} + Tl_{(s)} \quad (5)$$

$$MCl_{2(am)} + Na_2S_{(am)} \rightarrow MS_{(s)} + 2NaCl_{(s)}\ (M = Ni, Zn, Cd, Hg) \quad (6)$$

$$HgCl_{2(am)} + Na_2E_{(am)} \rightarrow HgE_{(s)} + 2NaCl_{(s)}\ (E = Se, Te) \quad (7)$$

$$2CuBr_{(am)} + Na_2S_{(am)} \rightarrow Cu_2S_{(s)} + 2NaBr_{(s)} + Cu_{2-x}S_{(s)}\ (x = 0.1, 0.2) \quad (8)$$

$$CuCl_{2(am)} + Na_2S_{(am)} \rightarrow CuS_{(s)} + 2NaCl_{(s)} + Cu_{2-x}S_{(s)}\ (x = 0.2) \quad (9)$$

$$CuCl_{2(am)} + Na_2Se_{(am)} \rightarrow CuSe_{(s)} + CuSe_{2(s)} + 2NaCl_{(s)} \quad (10)$$

$$CuCl_{2(am)} + Na_2Te_{(am)} \rightarrow CuTe_{1-x(s)}* + xTe_{(s)} + 2NaCl_{(s)} \quad (11)$$

[*In eq 11, two phases of nonstoichiometric (tellurium-deficient) copper(II) telluride were characterized by XRD: $Cu_{2.72}Te_2$ and Cu_4Te_3.]

In all cases (2)−(11), X-ray powder diffraction analysis of the preannealed material showed the presence of crystalline alkali metal halide. Washing of the product with CS_2 and water resulted in removal of the coproduced salt and isolation of single-phase metal chalcogenides. IR studies of the washed products showed absorptions characteristic of the desired material with broad bands centered at 600−150 cm^{-1}; no N−H stretches were observed. Annealing of the X-ray amorphous chalcogenides at 250−300 °C for 2−48 h induced sufficient crystallinity for analysis by X-ray powder diffraction. Energy-dispersive analysis by X-rays (EDAX) of the unwashed solids showed regions of sodium halide (NaCl, NaBr) as well as the metal chalcogenide. Trituration with water and CS_2 removed the co-formed salt, leaving only metal chalcogenide. Composition analysis both by electron-probe line analysis and by EDAX spot analysis were in agreement with the products identified by X-ray diffraction (within 1−2%); see Table 4. SEM of the as-formed powders showed submicron roughly spherical particles of size ca. 200 nm (Figure 1). Annealing of the samples encouraged particle agglomeration.

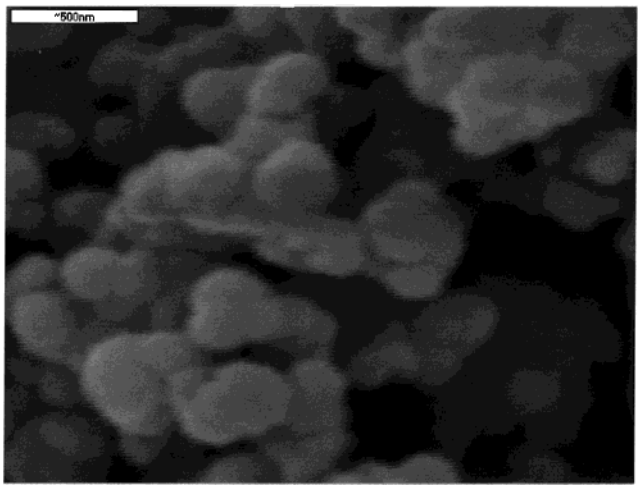

Figure 1. Scanning electron micrograph of triturated Ag_2S synthesized from the reaction of Na_2S and AgF in liquid ammonia, 25 °C, 36 h.

Raman patterns were obtained from the as-formed solids and the triturated materials. These showed bands that were diagnostic of the required material. This is illustrated in Figure 2 for ZnS. The band gap measurements of the metal chalcogenides were also determined by optical measurements; these showed evidence for blue shifts corresponding with nanoparticle formation. The laser induced fluorescence spectra of CdS showed a marked shift to higher frequency compared to bulk CdS (480 nm); see Figure 3.

Reactions involving lead and silver salts produced crystalline metal chalcogenides at room temperature in familiar mineral forms without recourse to annealing (Table 1). Figure 4 shows the XRD pattern obtained for the triturated, as-formed PbSe and PbTe products. Reaction of a 2:1 ratio of TlCl and Na_2E in liquid ammonia afforded crystalline thallium chalcogenides, $Tl^{I}[Tl^{III}E_2]$ (E = S, Se), and thallous telluride, $Tl_{2-x}E$ ($x = 1$; E = Te).

Synthesis of cupric and mercuric chalcogenides by metathesis reactions in ammonia, as well as the sulfides of nickel, zinc, cadmium, and copper(I), afforded X-ray powder diffraction patterns for the coproduced salt (NaCl or NaBr) only, with no evidence of crystalline metal chalcogenide, (6)−(11). Washing the X-ray amorphous chalcogenide materials with CS_2 and water followed by annealing at 250 °C for 48 h produced crystalline material (Table 2). The X-ray diffraction patterns of ZnS (Figure 5), CdS (Figure 6), HgS, and HgSe showed significantly broadened peaks indicative of the formation of nanometer particles. The Scherrer equation[31] gave particle sizes of 10 (ZnS), 39 (CdS), 24 (HgS), and 53 nm (HgSe).

(28) (a) Kher, S. S.; Wells, R. L. *Chem. Mater.* **1994**, *6*, 2056. (b) Carmalt, C. J.; Morrison, D. E.; Parkin, I. P. *J. Mater. Chem.* **1998**, *8*, 2209.
(29) Chianelli, R. R.; Dines, M. B. *Inorg. Chem.* **1978**, *17*, 2758.
(30) Bley, R. A.; Kauzlarich, S. M. *J. Am. Chem. Soc.* **1996**, *118*, 12461.

Table 3. XRD Data for Binary Transition Metal Pnictides Synthesized by Liquid Ammonia Mediated Metathesis Reactions at Room Temperature

reagents[a]	XRD of prewashed mater	product color	phases obtained after annealing washed mater[b]	lattice params, Å (± 0.01)	lit.[36] lattice params, Å
$3FeCl_2 + 2Na_3As$	NaCl	black	FeAs	$a = 5.39$, $b = 5.93$, $c = 3.27$	$a = 5.39$, $b = 5.93$, $c = 3.27$
$3FeCl_2 + 2Na_3Sb$	NaCl	black	FeSb	M	
$3CoCl_2 + 2Na_3As$	NaCl	black	CoAs (orthorhombic)	$a = 3.46$, $b = 5.87$, $c = 5.29$	$a = 3.46$, $b = 5.87$, $c = 5.29$
$3CoCl_2 + 2Na_3Sb$	NaCl	black	CoSb (hexagonal)	$a = 3.88$, $c = 5.19$	$a = 3.88$, $c = 5.19$
$3NiCl_2 + 2Na_3As$	NaCl	black	NiAs (hexagonal) + [Ni]	$a = 3.62$, $c = 5.01$	$a = 3.62$, $c = 5.01$
$3NiCl_2 + 2Na_3Sb$	NaCl	black	NiSb (hexagonal) + [Ni]	$a = 3.93$, $c = 5.13$	$a = 3.93$, $c = 5.13$
$3ZnCl_2 + 2Na_3As$	NaCl	black	Zn_3As_2 + [Zn, As]	$a = c = 5.81$	$a = c = 5.81$
$3ZnCl_2 + 2Na_3Sb$	NaCl	black	Zn_3Sb_2 + [Zn, Sb]	M	
$3CdCl_2 + 2Na_3As$	NaCl	black	Cd_3As_2 + [Cd, As]	$a = 8.93$, $c = 12.68$	$a = 8.93$, $c = 12.68$
$CdCl_2 + 2Na_3Sb$	NaCl	black	Cd_3Sb_2 + [Cd, Sb]	M	

[a] Reagents (expressed with molar ratios) stirred in liquid ammonia at room temperature for 36 h. [b] Phases characterized by X-ray powder diffraction *after* annealing at 250−300 °C for 48 h. All minor phases (< ca. 10 %) represented by square brackets.

Table 4. SEM/EDXA Data of Binary Metal Chalcogenides Synthesized by Metathetical Reaction in Liquid Ammonia at Room Temperature

		ratio of elements[c] (exptl error ± 2−3 atom %)		
reagents[a]	particle morphology[b]	elem. ratio	exptl values	theor values
$NiCl_2 + Na_2S$	1−5 μm aggregates; irregular particles < 50 nm	Ni:S	50:50	50:50 (NiS)
$ZnCl_2 + Na_2S$	1−5 μm aggregates; spherical particles < 50 nm	Zn:S	50:50	50:50 (ZnS)
$CdCl_2 + Na_2S$	1−5 μm aggregates; spherical particles < 50 nm	Cd:S	50:50	50:50 (CdS)
$2CuBr + Na_2S$	1−8 μm aggregates; irregular particles < 100 nm	Cu:S	67:33	67:33 (Cu_2S)
		Cu:S	64:36	$Cu_{2-x}S$ (2 phases)
$CuCl_2 + Na_2S$	1−8 μm aggregates; spherical particles < 100 nm	Cu:S	50:50	50:50 (CuS)
		Cu:S	67:33	67:33 (Cu_2S)
$CuCl_2 + Na_2Se$	1−8 μm aggregates; irregular particles < 100 nm	Cu:Se	50:50	50:50 (CuSe)
$CuCl_2 + Na_2Te$	1−8 μm aggregates; spherical particles < 100 nm	Cu:Te	42:58	Cu_4Te_3 (2 phases)
$2AgF + Na_2S$	1−5 μm aggregates; spherical particles < 50 nm	Ag:S	67:33	67:33 (Ag_2S)
$2AgF + Na_2Se$	1−5 μm aggregates; spherical particles < 50 nm	Ag:Se	67:33	67:33 (Ag_2Se)
$2AgF + Na_2Te$	1−5 μm aggregates; spherical particles < 50 nm	Ag:Te	67:33	67:33 (Ag_2Te)
$HgCl_2 + Na_2S$	1−5 μm aggregates; spherical particles < 50 nm	Hg:S	50:50	50:50 (HgS)
$HgCl_2 + Na_2Se$	1−5 μm aggregates; spherical particles < 50 nm	Hg:Se	50:50	50:50 (HgSe)
$HgCl_2 + Na_2Te$	1−5 μm aggregates; spherical particles < 50 nm	Hg:Te	50:50	50:50 (HgTe)
$2GaCl_3 + 3Na_2S$	1−5 μm aggregates; spherical particles < 50 nm	Ga:S	40:60	40:60 (Ga_2S_3)
$2GaCl_3 + 3Na_2Se$	1−5 μm aggregates; spherical particles < 50 nm	Ga:Se	40:60	40:60 (Ga_2Se_3)
$2GaCl_3 + 3Na_2Te$	1−5 μm aggregates; spherical particles < 50 nm	Ga:Te	40:60	40:60 (Ga_2S_3)
$2InCl_3 + 3Na_2S$	1−5 μm aggregates; spherical particles < 50 nm	In:S	40:60	40:60 (In_2S_3)
$2InCl_3 + 3Na_2Se$	1−5 μm aggregates; spherical particles < 50 nm	In:Se	40:60	40:60 (In_2Se_3)
$2InCl_3 + 3Na_2Te$	1−5 μm aggregates; spherical particles < 50 nm	In:Te	40:60	40:60 (In_2S_3)
$2TlCl + Na_2S$	1−8 μm aggregates; irregular particles < 200 nm	Tl:S	50:50	50:50 (TlS)
$2TlCl + Na_2Se$	1−8 μm aggregates; irregular particles < 200 nm	Tl:Se	50:50	50:50 (TlSe)
$2TlCl + Na_2Te$	1−8 μm aggregates; irregular particles < 200 nm	Tl:Te	63:37	63:37 (Tl_5Te_3)
$PbCl + Na_2S$	1−5 μm aggregates; spherical particles < 50 nm	Pb:S	50:50	50:50 (PbS)
$PbCl + Na_2Se$	1−5 μm aggregates; spherical particles < 50 nm	Pb:Se	50:50	50:50 (PbSe)
$PbCl + Na_2Te$	1−5 μm aggregates; spherical particles < 50 nm	Pb:Te	50:50	50:50 (PbTe)
$3MCl_2 + 3Na_3Pn$[d]	1−5 μm aggregates; irregular particles 50−100 nm	M:Pn[e]	60:40	40:60 (M_3Pn_2)
$3MCl_2 + 3Na_3Pn$[f]	1−8 μm aggregates; irregular particles 50−100 nm	M:Pn[e]	60:40	40:60 (M_3Pn_2)

[a] Molar ratios of reagents given for the room-temperature, liquid ammonia metathesis reaction of transition metal halides with sodium chalcogenides. Subsequent analyses were obtained from samples *washed* with distilled water, and refer to both preannealed and annealed material (unless stated). [b] Assessed by SEM at maximum magnification. [c] Elemental composition of phase assessed by EDXA (spot size 1 μm). Approximately surface abundance of multiple phases (assessed qualitatively using backscattered electrons) is expressed either as a percentage or as *major*/*minor* phases. [d] M = Fe, Co, Ni; Pn = As, Sb. [e] Free elements (M, Pn) detected as minor phase. [f] M = Zn, Cd; Pn = As, Sb.

Equation 12 describes the synthesis of X-ray amorphous group 13 sesquichalcogenides. As before, annealing of the isolated product at 250−300 °C for 2−48 h induced sufficient crystallinity for X-ray characterization of the powders (Table 2).

$$2MCl_{3(s)} + 3Na_2E \rightarrow M_2E_{3(s)} + 6NaCl_{(s)} \quad (M = Ga, In; E = S, Se, Te) \quad (12)$$

Interestingly, annealing the selenide/telluride material in the presence of oxygen afforded a metal chalcogenate (rather than a metal oxide) with retention of the metal to chalcogen composition (2:3):

$$M_2E_{3\,(s)} + 4.5O_{2\,(g)} \rightarrow M_2E_3O_{9\,(s)} \quad (M = Ga, In; E = Se, Te) \quad (13)$$

Prior to annealing the product from the metathesis of tin(II) or tin(IV) halides and sodium chalcogenides showed only crystalline ammonium halide by X-ray powder diffraction. This suggests that tin halide reactions are indicative of the lighter group 14 halides (Ge, Si) in preferentially undergoing ammonolysis upon addition to liquid ammonia rather than a metathetical reaction. It is well documented that silicon tetrahalides undergo sequential ammonolysis in liquid ammonia, affording $Si(NH)(NH_2)_2$ up to 100 °C in conjunction with four

(31) (a) Bawendi, B. M.; Kortan, A. R.; Steigerwald, M. L.; Brus, L. E. *J. Chem. Phys.* **1989**, *91*, 7282. (b) West, A. R. *Solid State Chemistry and its Applications*; J. Wiley and Sons: Chichester, 1992; p 174.

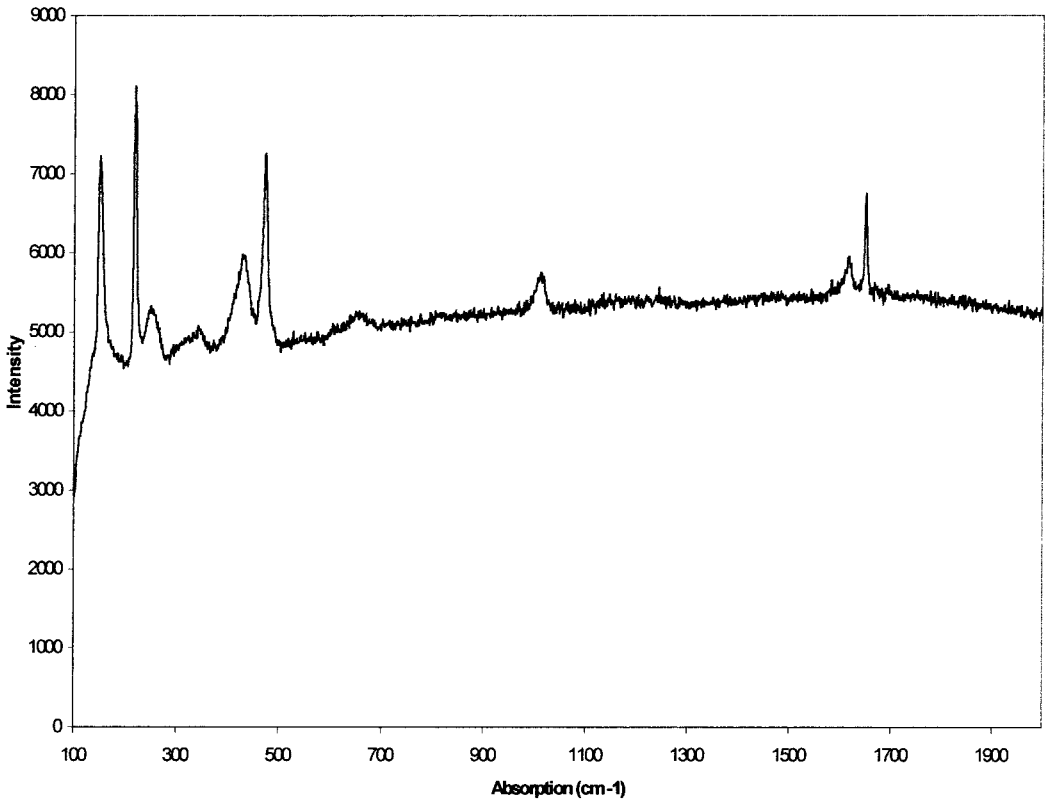

Figure 2. Raman pattern for ZnS made from reaction of $ZnCl_2$ and Na_2S in liquid ammonia, 25 °C, 36 h.

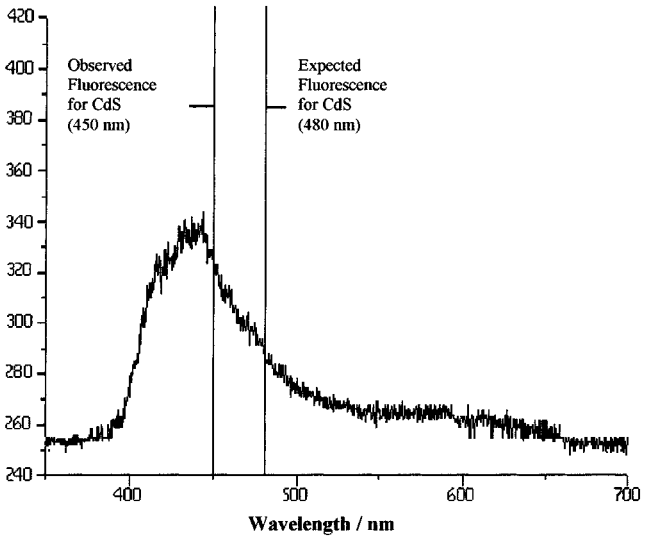

Figure 3. Laser induced fluoresence spectra of CdS synthesized from reaction of $CdCl_2$ and Na_2S in liquid ammonia, 25 °C, 36 h.

molar equivalents of ammonium halide (eqs 14 and 15).[32]

$$SiCl_4 + 8NH_3 \rightarrow Si(NH_2)_4 + 4NH_4Cl \quad (14)$$

$$Si(NH_2)_4 \rightarrow SiNH(NH_2)_2 + NH_3\ 0\ °C \leq T \leq 100\ °C \quad (15)$$

Pnictides of Iron, Cobalt, and Nickel: Synthesis and Characterization. Stoichiometric quantities of MCl_2 (M = Fe, Co, Ni) and Na_3Pn (Pn = As, Sb) were stirred in liquid ammonia for 36 h at room temperature. Each product was observed to be inhomogeneous, containing both white and black material. XRD analysis prior to workup showed the presence of only alkali metal halide (NaCl), suggesting that a metathetical reaction had taken place. After repeated washings with distilled water, a black material was isolated and shown to be X-ray amorphous. EDXA of the isolated black material showed the presence of two phases: metal pnictide and a minority metal phase. SEM analysis using backscattered electrons enabled the mixed phases to be quantified; typically micron-sized particles of each phase were observed. These phases showed little change in either number or distribution after annealing the samples at 250−300 °C for 48 h. However, XRD analysis of the annealed samples showed the presence of a single binary pnictide phase which was fully characterized as MPn (M = Ni, Co, Ni; Pn = As, Sb); see Table 3. In most of the XRD patterns the free metal was not seen; however, its presence in the annealed powder was confirmed by EDAX. Presumably the low temperature annealing conditions employed were suitable to encourage crystallization of the metal chalcogenide but not the co-formed metal. In the NiAs and NiSb samples XRD analysis did show minor peaks associated with nickel metal. A combination of the XRD and EDAX results indicates that the reaction proceeds in accordance with eq 16.

$$3MCl_{2(s)} + 2Na_3Pn_{(s)} \rightarrow 2MPn_{(s)} + 6NaCl_{(s)} + M_{(s)} \quad (M = Co, Fe, Ni; Pn = As, Sb) \quad (16)$$

Group 12 Pnictides (Zn_3Pn_2 and Cd_3Pn_2): Synthesis and Characterization. XRD analysis of the products from reaction of MCl_2 and Na_3Pn also showed a mixture of coproduced salt (NaCl) and black, X-ray amorphous material. SEM/EDAX of the isolated black material showed variable elemental composition resulting from the presence of three intimately mixed phases, whose relative distributions seemed unaffected by annealing at 250−300 °C for 48 h. XRD analysis of the annealed material showed the presence of a single binary metal pnictide

(32) Billy, M. *Ann. Chim. (Paris)* **1959**, *4*, 795. Billy, M. *Compt. Rend.* **1958**, *246*, 433.

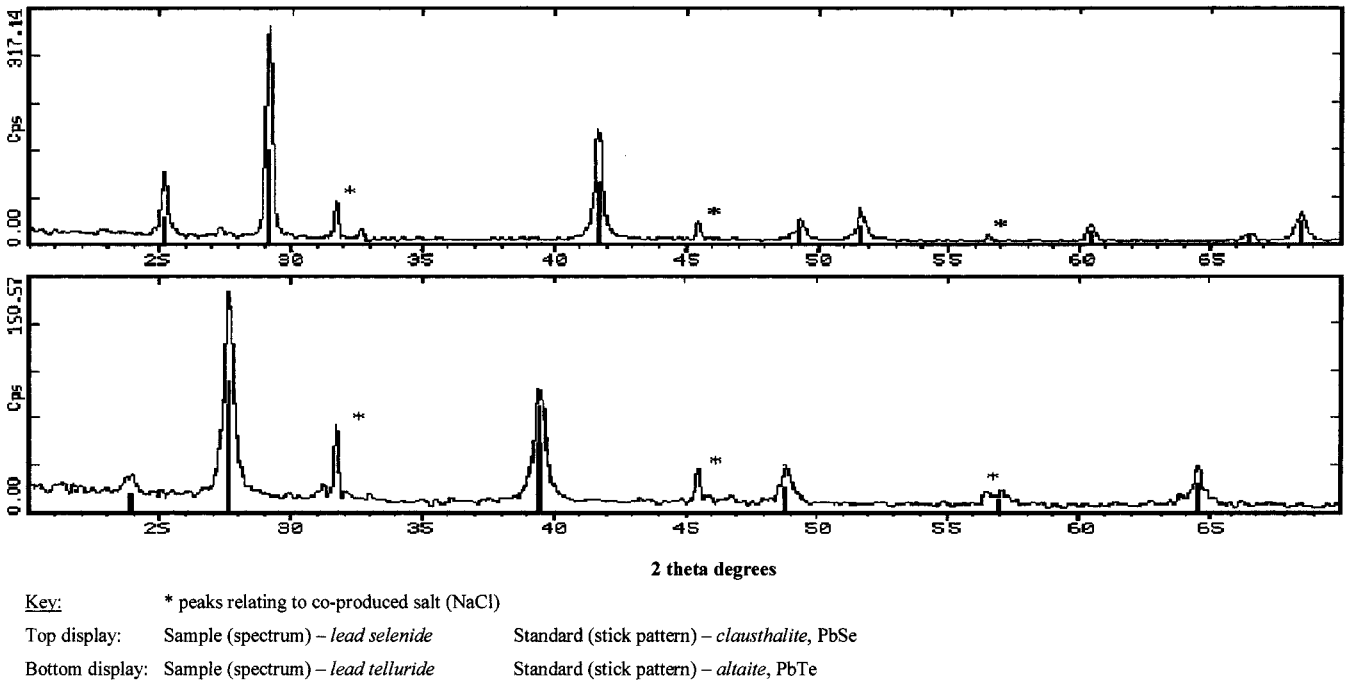

Figure 4. X-ray powder diffraction patterns of (i, top trace) product from the reaction of $PbCl_2$ and Na_2Se in liquid ammonia, 25 °C, 36 h, where stick pattern is for PbSe (clausthalite); (ii, bottom trace) product from the reaction of $PbCl_2$ and Na_2Te in liquid ammonia, 25 °C, 36 h, where stick pattern is for PbTe (altaite). * indicates co-formed NaCl.

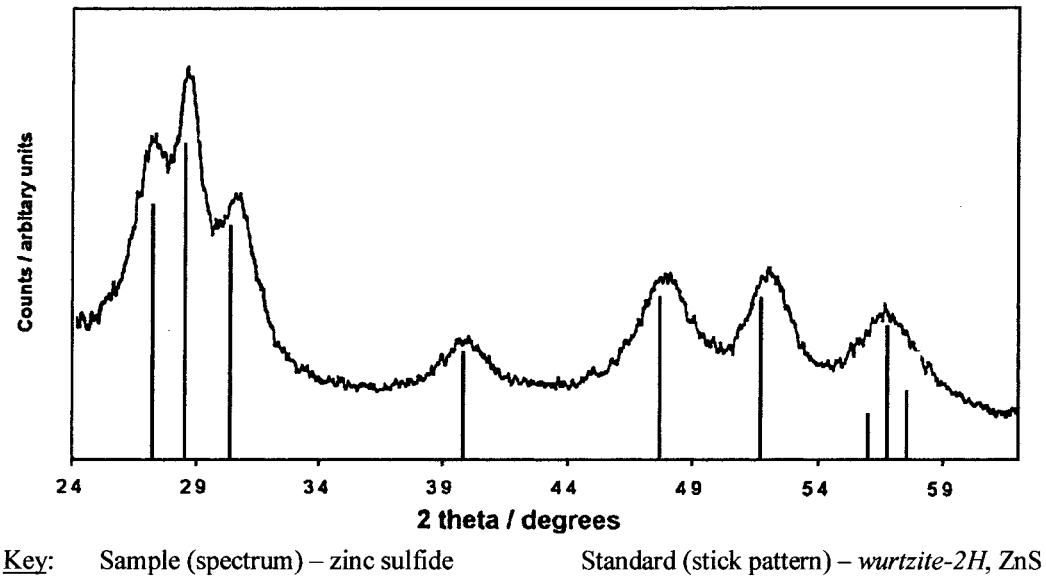

Figure 5. X-ray powder diffraction pattern of ZnS synthesized from reaction of $ZnCl_2$ and Na_2S in liquid ammonia, 25 °C, 36 h. Product was triturated with water and CS_2 and annealed at 250 °C for 2 h. Crystallite size of 100 Å from line broadening studies. Stick pattern for wurtzite-2H ZnS.

(of stoichiometry M_3Pn_2), in addition to both elemental metal and pnictogen (as described by eq 17).

$$3MCl_{2(s)} + 2Na_3Pn_{(s)} \rightarrow (1 - x)M_3Pn_{2(s)} + 2NaCl_{(s)} + (3 - x)M_{(s)} + (2 - x)Pn_{(s)} \quad (M = Zn, Cd; Pn = As, Sb) \quad (17)$$

Discussion

Reaction Scope. A wide range of binary metal chalcogenides and pnictides can be synthesized from the reaction, at room temperature, of metal halides and Na_2E/Na_3Pn in liquid ammonia. In most cases the products were the most thermodynamically stable forms, often in common mineral modifications. However, in the case of mercury sulfide (eq 6) the presence of only β-HgS after annealing (2 h, 250 °C), a less thermodynamically stable phase than the more common α-HgS,[8] suggests kinetic phases can be obtained in some metathetical reactions. The chalcogenides that could be synthesized were restricted to group 10−14 elements. Attempts at using group 6 salts such as $MoCl_5$ to form MoS_2 in ammonia resulted in destruction of the containment vessel. The reaction was repeated on three occasions, and in each attempt the reaction was too exothermic for the thick-walled containment vessel, resulting in vessel cracking and loss of ammonia. It is possible that the particle sizes of the metal halides play a dominant role in determining the course of the reaction, and care should be taken in repeating some of these reactions with very finely divided reagents.

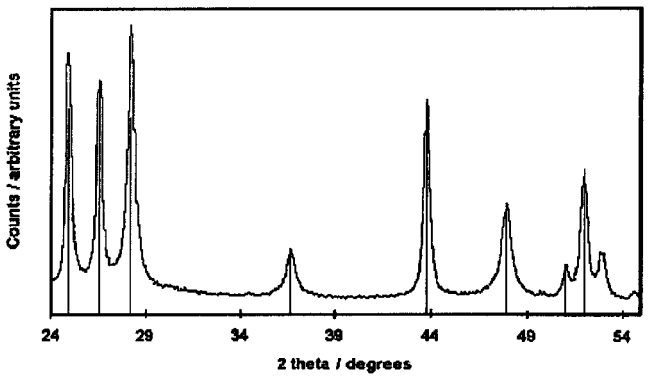

Key: Sample (spectrum) – cadmium sulfide Standard (stick pattern) – *greenockite*, CdS

Figure 6. X-ray powder diffraction pattern of CdS synthesized from reaction of $CdCl_2$ and Na_2S in liquid ammonia, 25 °C, 36 h. Product was triturated with water and CS_2 and annealed at 250 °C for 2 h. Crystallite size of 240 Å from line broadening studies. Stick pattern for greenockite CdS.

We have tried to extend the scope of the ammonia-mediated SSM reaction to metal phosphides. A wide variety of transition metal halides were reacted with sodium and lithium phosphides in liquid ammonia at room temperature. In no case was there evidence for a direct metathesis reaction. For example, no co-formed salt was found and unreacted metal halide was obtained from the reaction. We can see no thermodynamic reason for these reactions to fail as the comparable SSM reaction is known to form phosphide products. Further investigations in this system are underway.

Recent developments in metathesis reactions have resulted in a variety of mediating solvents, such as toluene, glyme ethers, benzene, and THF, being studied at reflux.[35] To date, liquid ammonia offers the only room temperature route to metathesis reactions. It is restricted in some respects through the formation of kinetically stable ammonia adducts of some of the metal halide precursors. For example, dissolution of both nickel and zinc bromide afforded $Ni(NH_3)_6Br_2$ and $Zn(NH_3)_2Br_2$, which persisted as unreacted reagents, even after annealing the reaction mixture. However, the corresponding insoluble nickel and zinc chlorides did react with sodium sulfide to form NiS and ZnS, respectively. Also, the tin halide precursors were shown to be unsuitable due to preferential ammonolysis reactions.

Reaction Mechanism. Solid state metathesis reactions have been speculated to proceed either via simple exchange of the ions or via elemental intermediates.[33] The presence of unreacted elements in the metal pnictide products, eqs 16 and 17, support an elemental recombination pathway with departure from a salt balanced equation and subsequent inhomogeneous products. In the metal chalcogenide reactions unreacted elements were not observed in the products.

Comparison with Solid State Metathesis Reactions. The metal chalcogenide materials reported here may be considered as products of solvent mediated metathetical reactions. Although the reactions were observed to be largely solid state in nature and their products comply with metathetical predictions, there are marked differences from purely solid state metathesis reactions. With SSM reactions, initiation of a region of the reaction mixture (typically by a localized heat source) results in sufficient heat being generated to either vaporize or liquefy most of the reagents and products.[33] Consequently, solid state diffusion is no longer rate limiting and the rate of reaction greatly exceeds the rate of heat dissipation. The high reaction temperature also expels volatile impurities.[23] Reactions observed in liquid ammonia metathesis proceed at room temperature without the need of an external heat source. It is possible that the liquid ammonia initiates the reactions by creating a change in state of the precursors, by dissolution of the disodium chalcodenide, or by formation of metallo−ammonia adducts. The reaction is likely to proceed both in the solid state, through surface-limited reactions, and in solution via solvent-mediated reactions. The solvent may serve to facilitate the reactions in two ways. Surface area of the reaction interface is greatly increased by the formation of solvated species. Furthermore, efficient stirring of insoluble reagents results in exposure of new reactive surfaces.

Product Morphology. Conducting the metathesis reactions in liquid ammonia rather than in the solid state produces greatly different product morphology. Completion of these highly exothermic reactions at room temperature shows the liquid ammonia to act as a heat sink. The high heat capacity of liquid ammonia allows efficient dissipation and absorption of reaction enthalpy, while the unreactive nature of the solvent toward the majority of precursors allows effective dispersion of insoluble particles. Consequently, product annealing is reduced and so particle size becomes restricted. This leads to the synthesis of nanocrystalline group 12−16 semiconductors (ZnS, CdS). Liquid ammonia metathesis affords spherical nanocrystallites agglomerated into aggregates of <1 μm, whereas SSM characteristically results in a fused mass—typically with sharp angles and faces—in excess of 10 μm in diameter.[23] In conventional solid state metathesis the product is invariably crystalline, whereas in the ammonia-mediated reactions crystallinity of the product is dependent on the specific reaction. Those that involve the most chalcophilic elements, silver, thallium, and lead, formed crystalline chalcogenides directly from the metathesis in ammonia. All of the other elements produced X-ray amorphous products that could be readily crystallized in a single step by facile heating (250−300 °C, 2−48 h). This route opens up the possibility for larger crystal growth with longer annealing times or slightly higher temperatures. Further such routes are likely to offer products with very low thermodynamic defect densities (although kinetic defects are still likely). The synthetic approach reported here not only requires less energy and processing time than conventional synthesis but can offer an effective, reproducible conversion from X-ray amorphous to crystalline materials.

We have not directly studied the effect of particle size of the reactants on the relative rates of the reactions. However, we did note that freshly formed finely divided reagents (Na_2S and Na_3As) did react quicker than those that had been left to agglomerate. It would be anticipated that higher surface area reagents would promote faster reactions. The minimum annealing temperatures required to induce crystallinity in the X-ray amorphous powders was not specifically determined. It was noted that 250 °C was sufficient in all of the systems reported here. It is possible that crystallinity could be induced at lower temperatures.

Conclusions

Solvent mediated metathesis reactions of metal halides and sodium chalcogenides and pnictides offer a simple route to a range of binary metal chalcogenides and pnictides. The reactions proceed at room temperature in liquid ammonia and can afford

(33) Bonneau, P. R.; Jarvis, R. F.; Kaner, R. B. *Inorg. Chem.* **1992**, *31*, 2127.
(34) Munir, Z. A.; Anselmi-Tamburini, U. *Mater. Sci. Rep.* **1989**, *3*, 277.
(35) Zavitsanos, P. D.; Morris, J. R. *Ceram. Eng. Sci. Proc.* **1983**, *4*, 624.
(36) Optional literature lattice parameters: *JCPDS Files, PDF2-Database*; International Center for Diffraction Data: Swarthmore, PA.

both crystalline and amorphous products together with co-formed salt. The salt is readily removed by trituration, and the amorphous products are crystallized by annealing at 250−300 °C. Solvent mediation produces nanometer-sized crystallites that are agglomerated into micron-sized particles; these particles are somewhat smaller than those formed by conventional solid state metathesis.

Experimental Section

All reagents (99.9% purity) were purchased from Aldrich Chemical Co. and used without further purification. Ammonia was purchased from BOC and used without drying. All manipulations were carried out in a dinitrogen-filled glovebox. Reactions were carried out using Schlenk techniques in thick-walled (3−4 mm), Teflon-in-glass, sealed Youngs-type tubes that were surrounded by safety netting. X-ray powder diffraction patterns were determined on a Siemens D5000 transmission powder diffractometer using germanium monochromated Cu $K\alpha_1$ radiation ($\lambda = 1.5405$ Å). They were indexed using either TREOR or METRIC-LS programs, with lattice parameters typically matched to within 0.02 Å of literature values. The SEM/EDXA measurements were determined on a JEOL JSM820 microscope, equipped with a Kevex Quantum Delta 4 detector and a Hitatchi SEM S-570 camera. The electron beam was focused (1 μm spot at surface) with an excitation energy of 20 keV. Electron-probe analyses were conducted on a JEOL EMA, using polished samples, and compared to metal and chalcogen standards. Infrared spectra were recorded on a Nicolet 205 spectrometer using KBr pressed disks. Raman spectra were recorded on a Dilor XY spectrometer. The 514.53 nm line of an argon laser (50 mW) was the excitation source; the slit width was 300 μm. Thermolysis studies were performed in a Lenton Thermal Designs tube furnace.

All reaction and product workup procedures were carried out in the manner described below for the zinc sulfide synthesis. Alkali metal chalcogenide was freshly prepared from direct combination of the elements in liquid ammonia. Condensation of the ammonia over either sodium sulfide or sodium selenide resulted in complete dissolution (partial dissolution of sodium telluride).

Preparation of Zinc Sulfide from the Reaction of Sodium Sulfide with Zinc Chloride. Ammonia (15 mL) was condensed over disodium sulfide (100 mg, 1.28 mmol) in a Youngs-type pressure tube at ca. −78 °C. Zinc chloride (175 mg, 1.28 mmol) was added. The tube was sealed and allowed to warm to room temperature with continuous magnetic stirring. Although liquid ammonia was observed to change color upon addition of the reagents, the zinc halide was not observed to dissolve in the ammonia. After 12−18 h the solution was cooled to −77 °C and the ammonia was evaporated under a nitrogen flow. Part of the product was triturated with 3×20 cm^3 of distilled water, typically yielding a black material, before being dried under vacuum. The isolated product was then annealed for 2 h at 250 °C. Product analysis (before and after annealing) involved XRD, SEM/EDXA (Table 4), and Raman, IR, and UV/vis spectroscopies (Tables 1−3). XRD analysis was also carried out on the prewashed product.

Caution! Liquid ammonia generates a pressure of about 7 atm at room temperature. Care should be exercised in the use of liquid ammonia in thick-walled glass vessels. All reactions should be conducted behind a safety screen with blast-proof netting around the reaction vessel. Reactions involving $MoCl_5$ and sodium chalcogenide and pnictides resulted in destruction of the containment vessel. Great care should be exercised in using very finely divided reagents in these syntheses.

Acknowledgment. The EPSRC is thanked for support of the Raman machine through Grant GR/M82592. D. Morrisen and C. Courtail are thanked for useful discussions.

IC010648S